Lucy Richardson and Mean Modified Wiener Filter for Construction of Super-Resolution Image

Original Scientific Paper

Pravin Balaso Chopade
Department of Electronics & Telecommunications,
M.E.S College of Engineering, Pune, India
pbchopade@mescoepune.org

Prabhakar N. Kota
Department of Electronics & Telecommunications,
M.E.S College of Engineering, Pune, India
Prabhukota1@gmail.com

Bhagvat D. Jadhav
Department of Electronics & Telecommunications,
JSPM's Rajarshi Shahu College of Engineering,
Pune, India
Bdjadhav_entc@jspmrscoe.edu.in

Pravin Marotrao Ghate
Department of Electronics & Telecommunications,
JSPM's Rajarshi Shahu College of Engineering,
Pune, India
pmghate_entc@jspmrscoe.edu.in

Shankar Dattatray Chavan
Department of Electronics & Telecommunications,
Dr. D. Y. Patil Institute of Technology, Pimpri, India
sdchavan73@gmail.com

Abstract *– The ultimate goal of the Super-Resolution (SR) technique is to generate the High-Resolution (HR) image by combining the corresponding images with Low-Resolution (LR), which is utilized for different applications such as surveillance, remote sensing, medical diagnosis, etc. The original HR image may be corrupted due to various causes such as warping, blurring, and noise addition. SR image reconstruction methods are frequently plagued by obtrusive restorative artifacts such as noise, stair casing effect, and blurring. Thus, striking a balance between smoothness and edge retention is never easy. By enhancing the visual information and autonomous machine perception, this work presented research to improve the effectiveness of SR image reconstruction The reference image is obtained from DIV2K and BSD 100 dataset, these reference LR image is converted as composed LR image using the proposed Lucy Richardson and Modified Mean Wiener (LR-MMWF) Filters. The possessed LR image is provided as input for the stage of bicubic interpolation. Afterward, the initial HR image is obtained as output from the interpolation stage which is given as input for the SR model consisting of fidelity term to decrease residual between the projected HR image and detected LR image. At last, a model based on Bilateral Total Variation (BTV) prior is utilized to improve the stability of the HR image by refining the quality of the image. The results obtained from the performance analysis show that the proposed LR-MMW filter attained better PSNR and Structural Similarity (SSIM) than the existing filters. The results obtained from the experiments show that the proposed LR-MMW filter achieved better performance and provides a higher PSNR value of 31.65dB whereas the Filter-Net and 1D,2D CNN filter achieved PSNR values of 28.95dB and 31.63dB respectively.*

Keywords*: bilateral total variation, fidelity term, lucy richardson filter, modified mean wiener filter, super-resolution*

1. INTRODUCTION

Technology in both software and hardware has advanced significantly during the past two decades. Industrial sectors have used modern technology to its fullest potential to produce electronic gadgets like computers, mobiles, Personal Digital Assistants (PDA), and countless gadgets at low prices [1]. To produce images with high quality, camera sensor manufacturing techniques have also advanced significantly. Digital sensors are designed to take a Low-Resolution (LR) image as an input and produce a High-Resolution (HR) image. The resulting HR image is anticipated to have sufficient edge information artifacts [2, 3]. Super-Resolution (SR) is a technique for generating high-quality images or frames from their low-quality counterparts utilizing digital image processing techniques. Applications of SR images are currently being used in academics and industry [4, 5]. SR is a developing field with a vast number of applications in electronic imaging, including forensics, surveillance, satellite imaging, and more [6]. The SR techniques utilize edge information to moderate the distorted problems in the tasks for obtaining super-resolution images. The SR techniques are categorized as the extraction of edges

and conversion of super-resolution images [7]. The SR technique is utilized to perform non-linear mappings among LR-HR images based on conventional super-resolution methods [8].

In real-time applications of SR imaging systems, numerous factors are responsible to lower the quality of the image. This is due to physical limitations, less count of image sensors, and a lower spatial rate for image sampling [9]. The SR technique is applied to the normal image sources to increase the image quality by adjusting contrast, saturation, etc [10]. The conversion of LR image to HR image is performed using super-resolution techniques such as Single Image Super-Resolution (SISR) and Multi-Image Super-Resolution (MISR). Among two techniques, SISR is widely used in the process of HR construction because it focuses on an individual LR image to provide a better result [11]. But, MISR can fill up the unavailable information by collecting the related data from other image sources. Conventionally, both techniques is utilized according to the user's needs [12, 13]. Many SR methods get the input of LR by relating it with degradation methods based on ground-truth images [14]. In some cases, the process of super-resolution is utilized to extract the information from LR images and achieve better results of spatial preservation [15,16]. In this paper, the quality of the reference LR image is enhanced using the proposed Modified Median Wiener Filter to overcome the issues related to image reconstruction process.

The main contribution of this research is listed as follows:

(i) The MMW filter cannot preserve the sharp features of the images (E.g. Lines). To overcome these drawbacks, the hybrid-MMW filter is proposed, which can preserve the sharp edges and eliminate the noise present in the image. Moreover, it smoothens the image by decreasing the intensity variations in the neighboring pixels and removing the blurred parts of the image.

(ii) The quality of the initial HR image is enhanced from the interpolation stage which is given as the input for the SR model.

(iii) The fidelity term is created to decrease the residual between the projected HR image and the detected LR image.

The remaining paper is organized as follows, Section 2 represents the related works of the paper. The proposed method is discussed in Section.3. The results and analysis are presented in Section 4. Finally, Section 5 represents the overall conclusion of the paper.

2. RELATED WORKS

This section provides related works on various filtering methods used to obtain SR images.

Park et al. [17] introduced a deep learning model consisting of 1D and 2D filters for SR of images. The 1D layer for extraction of features and 2D restoration layers of the image made up the suggested model. Using 1D filters, the first layer for extraction of features was created to separate parallel and perpendicular high-frequency signals. The second HR image-restoration layers were created to extract high-frequency signals by 2D filters. With the least amount of visual loss, the deep learning model was used to decrease the complexity of super-resolution methods. However, the model needed complex calculations and used more memory.

Luo et al. [18] introduced a lightweight Super-resolution model known as LatticeNet which utilized lattice blocks connected in series and backward feature fusion. The model combined multiple residual blocks by combinational co-efficient and this combinational co-efficient is present in any super-resolution block using residual blocks as a basic block. Moreover, backward fusion was utilized to combine information related to various fields. The structure of the lattice block consisted of two residual blocks in a linear combination that helped to increase the chance to attain a dominant network. However, the model can't be utilized in real-time applications and required more storage memory.

Esmaeilzehi et al. [19] introduced a Multiple spatial Range and Resolution level feature by generating a deep recursive Network (MuRNet) which initialized from the bicubic interpolated versions of images with low resolution and created high-quality super-resolved images. The introduced method combined multi-spatial range and level of resolution to provide enhanced maps of features in the framework of a recursive network. The MuRNet provided less count in the multiplied operations and improved the performance of the network. But the image was handled poorly, as it created an issue in the vanishing of gradient and lowered the overall performance of the super-resolution image.

Chen et al. [20] introduced a super-resolution image reconstruction technique based on an attention mechanism along with the feature map to enable images with low resolution to be super-resolute images. The reconstruction model contained three blocks for the extraction of features, the extraction of images, and a module to perform the reconstruction. The introduced technique increased the super-resolution effect of the image and improved the evaluation of quantitative objectives. However, the introduced technique performed slower in the reconstruction process due to its less capability.

Li et al. [21] introduced a deep adaptive information Filtering Network (Filter Net) to perform fast and accurate image Super-resolution. The introduced Filter Net could filter the information with low frequency from the adaptive features. The Filter Net contained dilated residual group with multi units of dilated residuals which improved the receptive field and exploited the information of low-resolution input. The Filter Net utilized an adaptive information fusion structure to construct weighted connections to increase the pixel-fitting capacity in the network. However, the consumption time was high and more memory space was occupied.

Gao and Zhou [22] introduced a Very Lightweight and Efficient Single Image Super Resolution (VLESR) method to balance the pixels of the image to get SR images. The VLESR technique utilized a Light Weight Residual Concatenation Block (LRCB) which propagates and fuses the local features of the image. Additionally, the Multi-way attention Block has the capability to integrate the features and enhance the quality of SR restoration of the image. However, the introduced VLESR did not contain any channel Concatenation and 1×1 convolution. If it's present it probably enhances the image accuracy.

He et al. [23] introduced an Orientation Aware feature extraction Model (OAM) that comprised a mixture of 1D and 2D kernels. In every OAM, the channel attention mechanism was employed to perform specific scene selections. The high-quality SISR combined both high-level and low-level features through progressive fusion Orientation method, which led to a concise execution of the SISR task.

3. LUCY RICHARDSON AND MEAN MODIFIED WIENER FILTER FOR CONSTRUCTION OF SUPER-RESOLUTION IMAGE

The presence of noisy and blurring effects are the general issues in SR images. A Bayesian framework is taken into consideration for implanting prior data into HR images to rectify this issue. The estimated vector is taken to be Gaussian because it is known that the HR image contains white Gaussian noise. MAP framework is used to solve the minimization problem as a result of the Bayes rule's procedure of creating the HR image. The first HR image is estimated via the conventional SR methodologies using bicubic or bilinear interpolation techniques on the reference LR image. However, LR image with low quality is obtained which leads to poor performance in the estimation of HR image. To overcome this issue and to obtain a composed LR image, the Median Modified Wiener Filter (LR-MMWF) is used. The composed LR image is fed into the bicubic interpolation to obtain the initial HR image. Then, the initial HR image is processed using the super-resolution model which consists of fidelity terms and regularization terms to provide the final HR image. The overall process involved in obtaining the SR image is represented in Fig. 1.

3.1. STEPS TO OBTAIN SUPER-RESOLUTION IMAGE

The process involved in the conversion of reference LR image into a super-resolution image using LR-MMWF involves various steps mentioned as follows:

(i) A series of low-resolution images are generated from the DIV2K dataset and BSD 100 which is considered as the input for the conversion process.

(ii) Assumption is made for one low-resolution image which is considered as reference LR image. The reference LR image is utilized to initialize the process to obtain a high-resolution image.

(iii) The angle of rotation, vertical and horizontal shifts that exist in the reference LR image is computed to improve the warp matrix of the image.

(iv) The process of conversion is employed in reference LR image to obtain the possessed LR image represented in Fig. 1. The composed LR image is given as the input for the stage of bicubic interpolation.

(v) The bicubic interpolation is applied to the possessed LR image to compute a high-resolution image at the initial stage. This initial resolution image is provided as an input for the stage of reconstruction of the image which is explained in section 3.1

(vi) The initial HR image is given as the input for the super-resolution model for image reconstruction. There the model computes the Fidelity term and regularization term using equation (6) and produces the final HR image as a super-resolution image.

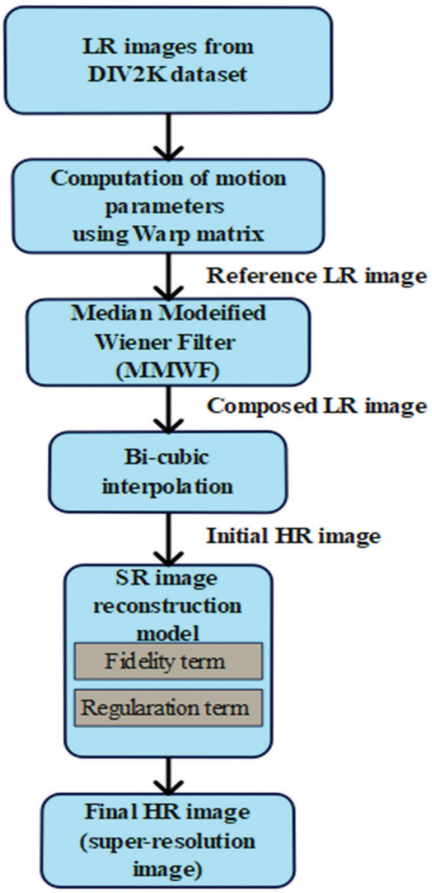

Fig. 1. Overall Process to Obtaining SR image

3.2. DATASET

The work is processed using two image datasets such as BSD100 [24] and DIV2K [25], and this section provides a brief description of these datasets. The Berkeley Segmentation Dataset 100 (BSD-100) consists of 100 images related to nature. A well-known image super-resolution dataset called DIV2K has 1,000 images of various scenarios, 800 of which are for training, 100 for validation, and 100 for testing. To promote research on image super-resolution with more realistic deterioration, it was gathered for the NTIRE2017 and NTIRE2018 Super-Resolution Challenges.

Low-resolution image with various sorts of degradations is included in this dataset. In addition to the typical bicubic downsampling, other degradations are taken into account while creating low-resolution images for the different challenge tracks. The three first images of the Div2K dataset and their corresponding gray and binary image in represented in Fig. 2 and some sample images from the BSD-100 dataset are provided in Fig. 3.

Fig. 2. The three first images of the Div2K dataset and their corresponding gray and binary image

Fig. 3. Sample images from the BSD-100 dataset

3.3. FRAMEWORK FOR SUPER-RESOLUTION IMAGES

The images obtained from the dataset are provided for the Bayesian framework to compute the possibility of the problem of uncertainty based on availed knowledge by conjoining various priors into a mathematical model that is capable of statistical implication. The Bayesian framework is used to estimate the likelihood of uncertainty problems depending on currently accessible knowledge. Hence, the uncertainty inference problem occurs in SR technology for evaluating projected HR images from a series of detected LR images. In other words, the observed LR image provides proof for the deduction of the HR image, and the reconstructed SR solution constrains the regularization term present in the image. SR reconstruction is equal to estimating the HR picture using provided LR images in the Bayesian framework. The Maximum Posteriori (MAP) technique, combines the image's prior constraints and produces outcomes by maximizing the probability cost function, which is a well-preferred one for the Bayesian framework. Additionally, it is known for its adaptability in the estimation of joint parameters and the preservation of edges. In general, rather than using the given parameters, Bayesian estimation is used to evaluate the probability distribution for unknown parameters. The function of the MAP estimator is mathematically defined using the equation (1)

$$\hat{X}_{MAP} = \arg max_X \prod_{k=1}^{M} P(Y_k|X).P(X) \quad (1)$$

Where the probability conditions of low-resolution images (Y_k) from the HR image (X) are represented as $P(Y_k \mid X)$ and the probability of the HR image at the prior condition is represented as $P(X)$.

The significant structure of SR consists of fidelity term and term of regularization. The MAP estimator is applied for reduction of residues among the HR image and LR image. Regularization is performed to improve the stability of the HR image. The mathematical form of the super-resolution framework is represented in equation (2).

$$\hat{X} = \arg min_X \sum_{k=1}^{N} \rho(DHF_k X - Y_k) + \lambda R(X) \quad (2)$$

Where the term data fidelity is represented as $\rho(DHF_k X\text{-}Y_k)$, the term of regularization is denoted as $R(X)$, and the parameter of regularization is represented as λ.

3.4. CONVERSION OF REFERENCE LR IMAGE TO COMPOSED LR IMAGE

The Bayesian framework provides a reference LR image as an input for the conversion of the reference LR image into a composed LR image. The median filter and the proposed LR-MMWF are utilized to convert the reference LR image to a composed LR image. The initial high-resolution image is assessed via the method of bicubic interpolation by providing a possessed LR image as input. The median filter smoothens the image by decreasing the variation intensity among the nearby pixels and the Lucy Richardson filter is used in removing the blurred part of the image. To reduce the residual between the projected HR image and the detected LR image, the L_2 is used for the data-fidelity term. Finally, the minimized operation is limited to the stabilized condition of the created HR image using the BTV prior model. The process of converting a reference LR image into a combined LR image is represented in Fig. 4.

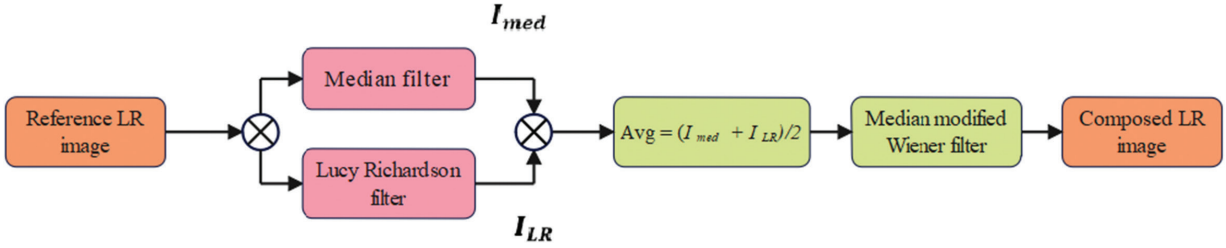

Fig. 4. Conversion of reference LR image to composed LR image

3.4.1. Hybrid of Lucy Richardson and Median Modified Wiener (LR-MMW) Filter

The reference image obtained from the Bayesian framework is processed using an LR-MMW filter to produce a composed LR image where the inhibited image quality is obtained. The widely utilized de-noising techniques in image processing are performed using linear filters (spatial filters). The spatial filter is based on the kernel's size which is generally referred to as a mask, it uses the intensity of the pixel to calculate the new pixel value. The median filters are less sensitive to extreme values, generally known as outliers. Moreover, the median filter efficiently neglects extreme values without affecting the image's sharpness. This advantage of the median filter is embedded with the advantage of the Wiener filter in producing edge-preserved images to make the MMW filter. Secondly, the Lucy Richardson filter is used in the process of de-blurring the image to provide an image with high resolution. The goal of the LR-MMWF strategy relies on increasing the quality of the image by de-noising the region of the background of a degraded image utilizing a median filter. This method is used to minimize the noise distribution in degraded images. Additionally, this method largely uses the Wiener filter to maintain the edge signal of the image. The LR-MMWF method is based on the Wiener filter and Lucy Richardson filter to reduce noise in the deteriorated image by replacing the value of pixels in the mask matrix along with median values. The average computed value in the Wiener filter gets interchanged by the value from the median filter. It is computed using equation (3) as follows:

$$b_{MMWF} = \bar{\mu} + \frac{\sigma^2 - v^2}{\sigma^2}.(a - \overline{\mu}) \quad (3)$$

Where $\bar{\mu}$ is the median value, the variance in the Gaussian noise of the image is represented as σ^2, and the variance of noise in the matrix of the Wiener filter is denoted as v^2. The area of every individual pixel is represented as a.

The benefit of employing the LR-MMWF technique is that the edge signal is better retained when compared to the usage of the median and Wiener filter techniques. This helps to improvise the quality of the deteriorated image using the drop-off effect. Regarding the de-noising effect, the LR-MMWF technique can significantly outperform traditional filters. In addition, it can simultaneously keep the edge signal and eliminate the background noise signal in the image.

3.5. RECONSTRUCTION OF IMAGE

The composed LR image obtained from a combination of LR-MMW filters is reconstructed to provide a super-resolution image from the HR image. Here the data fidelity term is represented as L_p and the regularization term is discussed using the model of BTV (Bilateral Total Variation). The data fidelity L_p is defined for the high-resolution image using equation (4).

$$F(X) = \arg min_X \sum_{k=1}^{N} (DHF_k X - Y_k) \quad (4)$$

where the motion and blur matrices are represented as D and H, and the movement of the matrices is denoted as F.

The BTV model is a combination of a bilateral filter with total variation, and it utilizes more neighbors to measure the gradient level for the provided pixels. Moreover, the sharp edges of the image are preserved using BTV model as it is low in cost and easy for implementation. The formula of BTV is mathematically represented in equation (5).

$$R_{BTV}(X) = \sum_{l=-P}^{P} \sum_{m=0}^{P} \alpha^{|m|+|l|} X - S_x^l S_y^m X_1 \quad (5)$$

Where the shifted HR image in the horizontal direction for l pixels is denoted as S_x^l and the shifted HR image in the vertical direction for m pixels is denoted as S_y^m (where $l+m \geq 0$). The scaling weight is represented as α which lies in the range of $0<\alpha<1$ and P is known as the controlled parameter.

The problem can be addressed in an infinite number of ways and under various circumstances. Additionally, minute levels of noise present in the measurements, cause significant agitations in the final solution, making it unstable. Therefore to arrive at a stable solution, artifacts are removed from the final solution, the convergence rate is improved, and the regularization method is used in SR image reconstruction. There are many regularization techniques, and one of them has is used to produce HR images with sharp edges and implementation simplicity as a primary advantage. In the picture reconstruction step, the regularization term is used to make up for missing data using some prior knowledge that is used to reduce loss. The regularization of BTV is formulated using equation (6)

$$X = arg\, min_X \left[\sum_{k=1}^{N} (DHF_k X - Y_k) + \lambda \sum_{l=-P}^{P} \sum_{m=0}^{P} \alpha^{|m|+|l|} X - S_x^l S_y^m X_1 \right] \quad (6)$$

The steepest descent method is utilized to obtain a fast convergence rate for the true HR image and it is assessed with less count of iterations. The iteration using the steepest descent method is computed by the formula in equation (7).

$$X_{n+1} = X_n - \beta \left[\sum_{K=1}^{N} F_K^T H^T D^T sign\left(DHF_k X_n - Y_K\right) + \lambda \sum_{l=-P}^{P} \sum_{m=0}^{P} \alpha^{|m|+|l|} \left[I - S_y^{-m} S_x^{-l} \right] sign\left(\hat{X}_n S_x^l S_y^m \hat{X}_n\right) \right] \quad (7)$$

Where the scalar unit which regulates size of the step in the gradient direction is represented as β and the parameter utilized for regularization is denoted as λ. The terms S_y^{-m} and S_x^{-l} represent the transposed matrices of S_y^m and S_x^l correspondingly.

4. RESULTS AND DISCUSSION

This section provides results obtained from the proposed LR-MMW filter for various metrics to evaluate image quality. The design and simulation of the LR-MMW filter can be performed using MATLAB software R2020a and system specifications with an Intel Core i7 processor with 8 GB RAM and a 64-bit Windows 10 operating system. The LR-MMW filter is utilized to provide

super-resolution images from the considered datasets such as DIV2K and BSD100 dataset. The performance of the LR-MMW filter is evaluated for parameters such as Peak-Signal-to-Noise Ratio (PSNR) and Structural Similarity Index (SSIM) to compute the quality of the image. The mentioned evaluation metrics (PSNR and SSIM) can be computed using equation (9) and equation (13) as follows

PSNR

The PSNR is one of the general methods to evaluate the image quality. It is usually described using Mean Square Error (MSE). The MSE for two $W \times H$ images X and Y is computed using the formula given in equation (8).

$$MSE = \frac{1}{WH}\sum_{i=0}^{W-1}\sum_{j=0}^{H-1}[X(i,j) - Y(i,j)]^2 \quad (8)$$

Hence, the PSNR is represented by equation (9)

$$PSNR = 10log\left(\frac{X_{MAX}^2}{MSE}\right) = 20\,log\left(\frac{X_{MAX}}{\sqrt{MSE}}\right) \quad (9)$$

Where the largest pixel value of the image is denoted as X_{MAX}.

SSIM

The structural similarity of the image is provided by the intensity $L(x, y)$ of the image, contrast of the image $C(x, y)$ and structure of the image $S(x, y)$.

The value of $L(x, y)$, C(x,y) and $S(x, y)$ is computed using the formula provided in the equation (10-12) as follows:

$$L(x,y) = (2\mu_x\mu_y + C_1)/(\mu_x^2 + \mu_y^2 + C_1) \quad (10)$$

$$C(x,y) = (2\sigma_x\sigma_y + C_2)/(\sigma_x^2 + \sigma_y^2 + C_2) \quad (11)$$

$$S(x,y) = (\sigma_{xy} + C_3)/(\sigma_x\sigma_y + C_3) \quad (12)$$

Where the reconstructed HR image is denoted as x and the original HR image is denoted as y. The mean and variance of the image are denoted as μ and σ respectively. The constants are denoted as C_1,C_2, and C_3 respectively.

Hence, the SSIM is defined using the equation (13) as follows:

$$SSIM(x,y) = L(x,y).C(x,y).S(x,y) \quad (13)$$

Where $L(x,y)$ is denoted as intensity of the image, $C(x,y)$ is denoted as contrast of the image, and the structure of the image is denoted as $S(x,y)$.

The input LR image and output SR image using Lucy Richardson and Mean Modified Wiener Filter are represented in Fig. 5 and Fig. 6 respectively. The size of the input LR image is 481×321 and the size of the output image is 850×641

Fig. 5. Input LR image from DIV2K dataset

Fig. 6. Output SR image from the DIV2K dataset

4.1. PERFORMANCE ANALYSIS

The performance of the proposed LR-MMW filter for the DIV2K and BSD100 datasets is described in this section. The performance is evaluated based on parameters such as Peak-Signal-to-Noise Ratio (PSNR) and Structural Similarity Index (SSIM). The performance is evaluated for the Kalman filter (KF), Wiener Filter (WF), Mean Modified Wiener Filter (MMWF), and the proposed LR-MMW filter. Table.1 represents the performance of the proposed MMWF filter for the DIV2K dataset.

Table 1. Performance of various filters for DIV2K dataset

Dataset	Filters	PSNR (dB)	SSIM
Diverse2K (DIV2K) dataset	Wiener Filter	21.43	0.784
	Kalman Filter	24.56	0.813
	MMW Filter	29.62	0.886
	LR-MMW Filter	31.69	0.92

As per Table 1, the performance of various filters to improve image quality is discussed by computing the parameters such as PSNR and SSIM.

The results obtained from Table 1 show that the proposed LR-MMW filter attained high PSNR and SSIM of 31.54 dB and 0.912 and provides an effective SR image from the DIV2K dataset. This better result is due to the presence of an image reconstruction model which consists of (L_2 Norm) and (BTV prior). The L_2 Norm lessens the residual in the predicted HR image and BTV improves the stable state of generated HR image. The graphical comparison of PSNR value for various filters including the proposed LR-MMW filter is represented in Fig. 7:

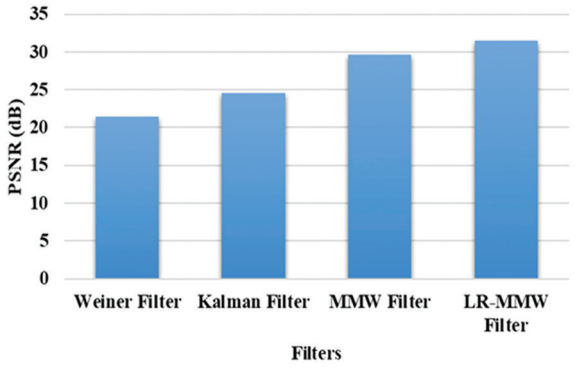

Fig. 7. Graphical representation of PSNR value for DIV2K dataset

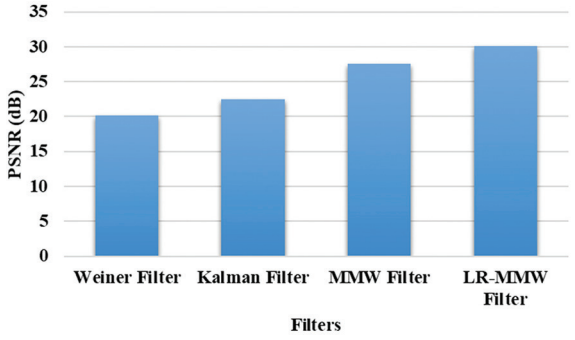

Fig. 8. Graphical representation of PSNR value for BDS 100 dataset

In Table 2 the performance of various filters to improve the image quality is discussed by computing the parameters such as PSNR and SSIM. The results obtained from Table 2 show that the proposed LR-MMW filter attained high PSNR and SSIM of 31.65 dB and 0.912 respectively for the BDS100 dataset and provides an effective super-resolution image. The graphical comparison of PSNR value for various filters including the proposed LR-MMW filter is represented in Fig. 8.

Table 2. Performance of various filters for the BDS 100 dataset

Dataset	Filters	PSNR (dB)	SSIM
Berkeley Segmentation Dataset (BSD-100)	Wiener Filter	20.12	0.762
	Kalman Filter	22.43	0.80
	MMW Filter	27.56	0.861
	LR-MMW Filter	31.65	0.91

Thirdly, the proposed LR-MMW Filter is evaluated to validate its efficacy for real-time images which are randomly collected based on a real-time environment. Table 3 mentioned below shows the efficiency of the proposed LR-MMW filter with the existing Wiener, Kalman and MMW filters by computing the value of PSNR and SSIM.

Table 3. Performance of various filters for the images obtained from real-time environment

Dataset	Filters	PSNR (dB)	SSIM
Images collected from real-time environment	Wiener Filter	25.93	0.745
	Kalman Filter	26.67	0.711
	MMW Filter	30.26	0.786
	LR-MMW Filter	33.71	0.831

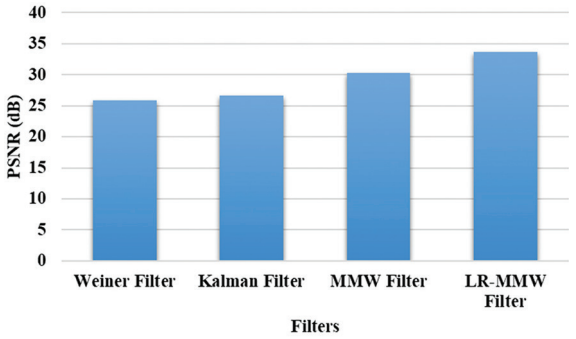

Fig. 9. Graphical representation of PSNR value for real-time images

The results from Table 3 and Fig. 9 show that the proposed LR-MMW filter is even effective for the data obtained from a real-time environment. While evaluating the PSNR value, the LR-MMW filter obtained a better PSNR value of 33.71 dB which is better than the existing Wiener, Kalman and MMW filters with 25.93 dB, 26.67dB, 30.26Db and 33.71dB respectively.

Overall, the LR-MMWF provides better PSNR and SSIM values DIV2K and BDS100 and the image obtained from a real-time environment, the better result is due to the utilized fidelity term and the regularization term in the image reconstruction model, and it increases the quality of the image and de-noising the region of background.

4.2. COMPARATIVE ANALYSIS

This section provides a comparison among various SR methodologies namely the Filter Net [16], 1D,2D-CNN filter [20] and the proposed LR-MMW filter. The values of PSNR and SSIM are evaluated for the BSD100 dataset based on the overall performance in providing SR images. The results obtained from the comparison show that the proposed LR-MMW attained better performance in the reconstruction of super-resolution images from the composed LR image. The LR-MMW method utilizes a multi-frame SR model which consists of fidelity terms (L_2 Norm) and regularization term (BTV prior). Moreover, the image obtained from the pro-

posed method attains better resolution than the existing methods. The graphical representation of PSNR and SSIM of LR-MMW with existing filter methods are represented in Fig. 9 and Fig. 10 respectively. Moreover, the comparative results for PSNR value and SSIM is shown in Table. 3 and Table. 4 respectively.

Table 4. Comparative table for PSNR

Filter methods	PSNR (dB)
1D,2D-CNN Filter [17]	31.63
Filter Net [21]	28.95
LR-MMW	31.65

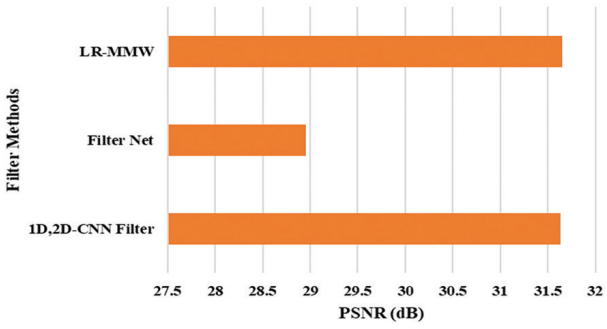

Fig. 10. Graphical representations of PSNR value

Table 4 and Fig. 10, it is shown that the proposed LR-MMW filter attains a high PSNR value of 31.65dB whereas the existing Filter Net and 1D, 2D CNN filter achieved PSNR values of 28.95 dB and 31.63 dB respectively. The presence of (L_2 Norm) and (BTV prior) present in the image reconstruction model help to obtain better PSNR values than the existing methodologies. This result is due to the presence of an image reconstruction model which consists of (L_2 Norm) and (BTV prior). The L_2 Norm reduces residues in the predicted HR image and BTV improves the stable state of generated HR image.

Table 5. Comparative table for SSIM

Filter methods	SSIM
1D,2D-CNN Filter [17]	0.726
Filter Net [21]	0.892
LR-MMW	0.914

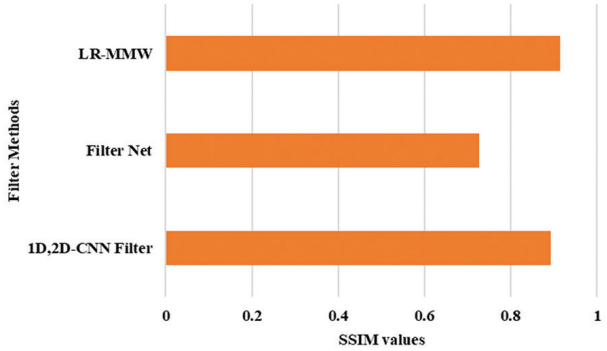

Fig. 11. Graphical representations of SSIM value

The above table.4 shows that the proposed LR-MMW attains higher structural similarity (SSIM) 0f 0.914 whereas the existing 1D,2D CNN filter, and Filter Net achieved SSIM of 0.892 and 0.726 respectively. The graphical representation of SSIM values is represented in Fig. 11.

From Table.4 and Table.5, it is concluded that the performance of the LR-MMW filter provides better PSNR and SSIM values compared with the existing filter methods. The LR-MMW filters the residues in the predicted HR image using L_2 Norm, and the stable state of the HR image is determined using the BTV model. Thus LR-MMW filter provides better performance by improvising the image quality and de-noising the background region effectively.

Moreover, the results are evaluated based on the spatial interpolation of the images obtained from Filter Net and LR-MMW filter. The images from the BSD 100 dataset with 3× upscaling are considered for evaluating the images whose sizes are 32×32, 64×64 and 128×128. Table 6 presents the outcome for varying image sizes for Filter Net and LR-MMW filter.

Table 6. Comparison of PSNR and SSIM by varying the pixel size of the images from the BSD100 dataset

Dataset	Size of the Image	PSNR (dB)		SSIM	
		Filter Net [21]	LR-MMW	Filter Net [21]	LR-MMW
BSD100 (3×upscaling)	32×32	28.45	33.78	0.7885	0.8128
	64×64	27.01	31.04	0.7179	0.7967
	128×128	27.05	30.97	0.7181	0.7342

The results from Table 6 show that the proposed LR-MMW achieved better interpolation for various image sizes obtained from BSD 100 dataset. For instance, the LR-MMW has obtained 31.04 Db for an image size of 64×64 which is comparatively higher than the existing Filter Net method. Similarly, SSIM value of LR-MMW is 0.7967 whereas Filter Net obtained 0.7179. These results prove the efficacy of the proposed LR-MMW filter and this better result is due to the bicubic interpolation which uses the 4×4 neighborhood method to determine the output.

5. CONCLUSION

This research proposed an LR-MMW filter to enhance the effectiveness of SR images to maximize both the analysis and human interpretation process. The results are evaluated based on the data collected from DIV2K and BSD 100 datasets, this research considered PSNR and SSIM to compute the efficiency of the proposed method. The benefit of employing the LR-MMW filter technique is that the edge signal is better retained when compared to the usage of the median and Wiener filter techniques. This helps to improvise the quality of the deteriorated image using the drop-off effect.

Regarding the de-noising effect, the LR-MMW filter technique can significantly outperform traditional filters. The performance of the proposed LR-MMW filter is evaluated with the Wiener, Kalman and MMW filters for both DIV2K and BSD 100 datasets. For DIV2K, the proposed LR-MMWF obtained PSNR of 31.69 dB and SSIM of 0.92 and for BSD 100 the value of PSNR and SSIM is 31.65dB and 0.91 respectively which is comparatively higher than the existing filter techniques. In the future, the proposed model can be implemented with deep learning techniques to obtain better results.

6. REFERENCES

[1] M. M. Khattab, A. M. Zeki, A. A. Alwan, B. Boualleague, S. S. Matter, A. M. Ahmed, "Regularized Multiframe Super-Resolution Image Reconstruction Using Linear and Nonlinear Filters", Journal of Electrical and Computer Engineering, Vol. 2021, 2021, p. 8309910.

[2] S. W. Remedios, S. Han, Y. Xue, A. Carass, T. D. Tran, D. L. Pham, J. L. Prince, "Deep filter bank regression for super-resolution of anisotropic MR brain images", Proceedings of the International Conference on Medical Image Computing and Computer-Assisted Intervention, Singapore, 18-22 September 2022, Vol. 13436, pp. 613-622.

[3] G. Suryanarayana, K. Chandran, O. I. Khalaf, Y. Alotaibi, A. Alsufyani, S. A. Alghamdi, "Accurate Magnetic Resonance Image Super-Resolution Using Deep Networks and Gaussian Filtering in the Stationary Wavelet Domain", IEEE Access, Vol. 9, 2021, pp. 71406-71417.

[4] M. V. Daithankar, S. D. Ruikar, "Analysis of the Wavelet Domain Filtering Approach for Video Super-Resolution", Engineering, Technology & Applied Science Research, Vol. 11, No. 4, 2021, pp. 7477-7482.

[5] W. Xu, H. Song, K. Zhang, Q. Liu, J. Liu, "Learning lightweight Multi-Scale Feedback Residual network for single image super-resolution", Computer Vision and Image Understanding, Vol. 197-198, 2020, p. 103005.

[6] V. Curcio, L. A. Alemán-Castañeda, T. G. Brown, S. Brasselet, M. A. Alonso, "Birefringent Fourier filtering for single molecule coordinate and height super-resolution imaging with dithering and orientation", Nature Communications, Vol. 11, 2020, p. 5307.

[7] K. Jonghyun, G. Li, I. Yun, C. Jung, J. Kim, "Edge and identity preserving network for face super-resolution", Neurocomputing, Vol. 446, 2021, pp. 11-22.

[8] Y. Huang, J. Li, X. Gao, Y. Hu, W. Lu, "Interpretable Detail-Fidelity Attention Network for Single Image Super-Resolution", IEEE Transactions on Image Processing, Vol. 30, 2021, pp. 2325-2339.

[9] I. Taghavi, S. B. Andersen, C. A. V. Hoyos, M. Schou, F. Gran, K. L. Hansen, M. B. Nielsen, C. M. Sørensen, M. B. Stuart, J. A. Jensen, "Ultrasound super-resolution imaging with a hierarchical Kalman tracker", Ultrasonics, Vol. 122, 2022, p. 106695.

[10] S. Aymaz, C. Köse, "A novel image decomposition-based hybrid technique with super-resolution method for multi-focus image fusion", Information Fusion, Vol. 45, 2019, pp. 113-127.

[11] Y. Chen, L. Liu, V. Phonevilay, K. Gu, R. Xia, J. Xie, Q. Zhang, K. Yang, "Image super-resolution reconstruction based on feature map attention mechanism", Applied Intelligence, Vol. 51, No. 7, 2021, pp. 4367-4380.

[12] X. Feng, J. Li, Z. Hua, "Guided filter-based multi-scale super-resolution reconstruction", CAAI Transactions on Intelligence Technology, Vol. 5, No. 2, 2020, pp. 128-140.

[13] F. Salvetti, V. Mazzia, A. Khaliq, M. Chiaberge, "Multi-image super resolution of remotely sensed images using residual attention deep neural networks", Remote Sensing, Vol. 12, No. 14, 2020, p. 2207.

[14] Y. Shi, H. Zhong, Z. Yang, X. Yang, L. Lin, "DDet: Dual-Path Dynamic Enhancement Network for Real-World Image Super-Resolution", IEEE Signal Processing Letters, Vol. 27, 2020, pp. 481-485.

[15] J. Cai, B. Huang, "Super-Resolution-Guided Progressive Pansharpening Based on a Deep Convolutional Neural Network", IEEE Transactions on Geoscience and Remote Sensing, Vol. 59, No. 6, 2021, pp. 5206-5220.

[16] J. Yang, Y.-Q. Zhao, J. C.-W. Chan, L. Xiao, "A Multi-Scale Wavelet 3D-CNN for Hyperspectral Image Super-Resolution", Remote Sensing, Vol. 11, No. 13, 2019, p. 1557.

[17] J. Park, J. Lee, D. Sim, "Low-complexity CNN with 1D and 2D filters for super-resolution", Journal of

Real-Time Image Processing, Vol. 17, No. 6, 2020, pp. 2065-2076.

[18] X. Luo, Y. Xie, Y. Zhang, Y. Qu, C. Li, Y. Fu, "LatticeNet: Towards Lightweight Image Super-Resolution with Lattice Block", Computer Vision – ECCV 2020, Lecture Notes in Computer Science, Vol. 12367, Springer International Publishing, 2020, pp. 272-289.

[19] A. Esmaeilzehi, M. O. Ahmad, M. N. S. Swamy, "MuRNet: A deep recursive network for super resolution of bicubically interpolated images", Signal Processing: Image Communication, Vol. 94, 2021, p. 116228.

[21] Y. Chen, L. Liu, V. Phonevilay, K. Gu, R. Xia, J. Xie, Q. Zhang, K. Yang, "Image super-resolution reconstruction based on feature map attention mechanism", Applied Intelligence, Vol. 51, No. 7, 2021, pp. 4367-4380.

[22] F. Li, H. Bai, Y. Zhao, "FilterNet: Adaptive Information Filtering Network for Accurate and Fast Image Super-Resolution", IEEE Transactions on Circuits and Systems for Video Technology, Vol. 30, No. 6, 2020, pp. 1511-1523.

[23] D. Gao, D. Zhou, "A very lightweight and efficient image super-resolution network", Expert Systems with Applications, Vol. 213, 2023, p. 118898.

[24] Z. He, D. Chen, Y. Cao, J. Yang, Y. Cao, X. Li, S. Tang, Y. Zhuang, Z. Lu, "Single image super-resolution based on progressive fusion of orientation-aware features", Pattern Recognition, Vol. 133, 2023, p. 109038.

[25] BSD100 dataset, https://www2.eecs.berkeley.edu/Research/Projects/CS/vision/bsds/BSDS300/html/dataset/images.html (accessed: 2023)

[26] DIV2K dataset, https://data.vision.ee.ethz.ch/cvl/DIV2K/ (accessed: 2023)